

Article

Dynamics of a Flexible Roof Test Model under Ambient Vibrations Measurements

Fabio Rizzo ^{1,2,*}, Chiara Bedon ³ , Sulyman Mansour ² , Aleksander Pistol ⁴, Maria Francesca Sabbà ² ,
Łukasz Flaga ⁴, Renata Klaput ⁴ and Dora Foti ² 

¹ Chair of Metal Structure L-3, Department of Civil Engineering, Cracow University of Technology, 31-155 Krakow, Poland

² Department of Architecture, Construction and Design, Polytechnic University of Bari, Via Orabona, 4, 70126 Bari, Italy; sulyman.mansour@poliba.it (S.M.); mariafrancesca.sabba@poliba.it (M.F.S.); dora.foti@poliba.it (D.F.)

³ Department of Engineering and Architecture, University of Trieste, 34127 Trieste, Italy; chiara.bedon@dia.units.it

⁴ Wind Engineering Laboratory, Cracow University of Technology, 31-155 Kraków, Poland; aleksander.pistol@pk.edu.pl (A.P.); lukasz.flaga@pk.edu.pl (Ł.F.); renata.klaput@pk.edu.pl (R.K.)

* Correspondence: fabio.rizzo@poliba.it

Abstract: Flexible roofs are sensitive to wind actions because they are light, and their deformability can induce local or global instability. In most cases, their design requires experimental wind tunnel testing to investigate the aeroelastic phenomena and the structural response under the wind. However, the reduced scale necessary in wind tunnels makes the dynamic identification of the test model difficult. Several approaches of multi-modal dynamic identification can be used, even if a specific approach is not defined for geometric nonlinear flexible roofs. Many times, the choice of the position of the sensors is affected by the unknown roof dynamics. This paper investigates the ambient vibration time-dependent accelerations for a flexible roof scaled model through Singular Value Decomposition (SVD) and their spatial correlations with the purpose of analyzing the signal structure and its acquisition to perform the dynamic identification of the test model.

Keywords: flexible roofs; random signals; singular value decomposition; eigenvectors; eigenvalues



Citation: Rizzo, F.; Bedon, C.; Mansour, S.; Pistol, A.; Sabbà, M.F.; Flaga, Ł.; Klaput, R.; Foti, D. Dynamics of a Flexible Roof Test Model under Ambient Vibrations Measurements. *Appl. Sci.* **2023**, *13*, 4135. <https://doi.org/10.3390/app13074135>

Academic Editor: Giuseppe Lacidogna

Received: 25 February 2023

Revised: 13 March 2023

Accepted: 20 March 2023

Published: 24 March 2023



Copyright: © 2023 by the authors. Licensee MDPI, Basel, Switzerland. This article is an open access article distributed under the terms and conditions of the Creative Commons Attribution (CC BY) license (<https://creativecommons.org/licenses/by/4.0/>).

1. Introduction

Vibration problems of structures and products have always been given attention in various industries, from the building sector to the different industrial fields. Modal analysis is a common method for dynamic property identification, including the predominant frequencies, the damping properties and the modal shapes. The aforementioned properties not only help in understanding the behavior of the studied object but also help in designing a structural control system capable of providing safe operating conditions. One such system of interest is the flexible roof (e.g., cable-net roof), which provides a common structural solution to cover relatively large areas mainly dedicated to social, musical or sports activities (e.g., mega conference halls or sports/music arena) [1–15]. Different advantages are usually guaranteed by the use of those roofing systems considering the consistent structural performance and their low self-weight characterized by the use of prefabricated elements that can be easily transported and mounted on site. Nevertheless, the proportionally lightweight to the wide area of the roofs makes them sensitive to the corresponding provoked wind actions even if they are neglected by codes [16–21]. Thus, particular attention should be given to both the stiffness and mass of the different components to assure the required dynamic characteristics [14,15].

Ambient vibration is one of the extensively used methods for the dynamic characterization of building and non-building structures in which time history registrations should

be accumulated from different monitoring points in which accelerometers are placed. Different techniques, either in the time domain or frequency domains, were developed and employed in recent years to identify the main properties of monitored systems [22,23]. The post-processing procedures become more complicated with the increase in monitored positions of structures, taking into account the high sampling rate and the single test durations that satisfy the processing procedure required to achieve a stable and meaningful mathematical solution from an engineering point of view. Shell structures expanding over large areas, such as a flexible roof, that are characterized by different close frequencies require an extensive network of monitoring points all over the various sections, which should increase the number of the three-axial accelerometers. Consequently, and due to the massive volume of the dataset collected during the performed free-vibration tests, the application of the classical method becomes very complicated and expensive from a computational point of view. One of the very recent solutions is to apply the Singular Value Decomposition (SVD) method to deal with big datasets of registrations effectively [24–31].

SVD is a high-powered technique that is classically (or mathematically) used to solve sets of matrix-form equations and is adoptable for complicated conditions in which classical methods such as LU decompositions and Gaussian elimination are not applicable or not capable of providing satisfying results or even in other cases where the number of unknowns is more or less than the number of the equations to be solved in which it can help in identifying the number of modes in each frequency response band of the corresponding transfer function in a stable way [24]. One of the main benefits of the method is the capability of separating and distinguishing the different modes produced in a single transfer function that corresponds to each mode without residual effects. Even if the typical transfer function is rarely clear of the effects of the nearby modes and the residual effects, at the same time, the Simplified single Degree Of Freedom (SDOF) system can accurately provide the resonance frequency and its corresponding damping ratio. In the last few years, the application of this method has become of interest in different fields, such as image processing, radar systems, etc., due to the reasonable computational cost guaranteed by this method in such complex real-time setting problems [24–31].

The work presented hereafter intends to highlight the potentiality of this method in the structural engineering sector, a field that is yet to commonly recognize its applicability, by investigating some aspects related to its capability of studying the dynamics of one of the most complicated systems in either the building or non-building fields of structures, which is the cable-net roof in this study.

The presented work is organized as follows: The first chapter introduces the case of flexible roofs, providing details on their differences from other structures and providing some other details on the scaling requirements for the experimental testing of those roofs. The second chapter describes the experimental campaign of the free vibration tests, indicating the monitored points and adopted instruments and the main characteristics of the raw results. The third chapter concerns the SVD application for identifying the dynamic properties of the roof specimen based on the time history registered during the ambient tests. Moreover, the same analysis is performed using the classical FDD method. Finally, the last chapter provides a comparison between the output of the two methods, highlighting different aspects and leading different related discussions.

2. The Case Study: A Tensile Structure Saddle Roof

The cable net with hyperbolic paraboloid shape [1–15] has two types of cables: upward (i.e., load bearing for gravitational loads) and downward cables (i.e., stabilizing for gravitational loads) under gravitational loads (Figure 1a). The former type increases its internal traction, while the latter decreases its internal traction. Under suction induced by wind (Figure 1b), it is the opposite. When the suction is non-uniformly distributed on the roof (Figure 1c), some problems may occur because some parts of the upward cable can be almost horizontal. This means that it loses its internal traction. This is very dangerous for the roof's global stability. At the same time, some parts of the downward cable exceed

the limit of traction, which can result in a breaking collapse because cables are made of harmonic steel, resulting in non-ductile elements. Finally, under extreme conditions of wind (Figure 1d), upward cables can invert their curvature, causing roof instability.

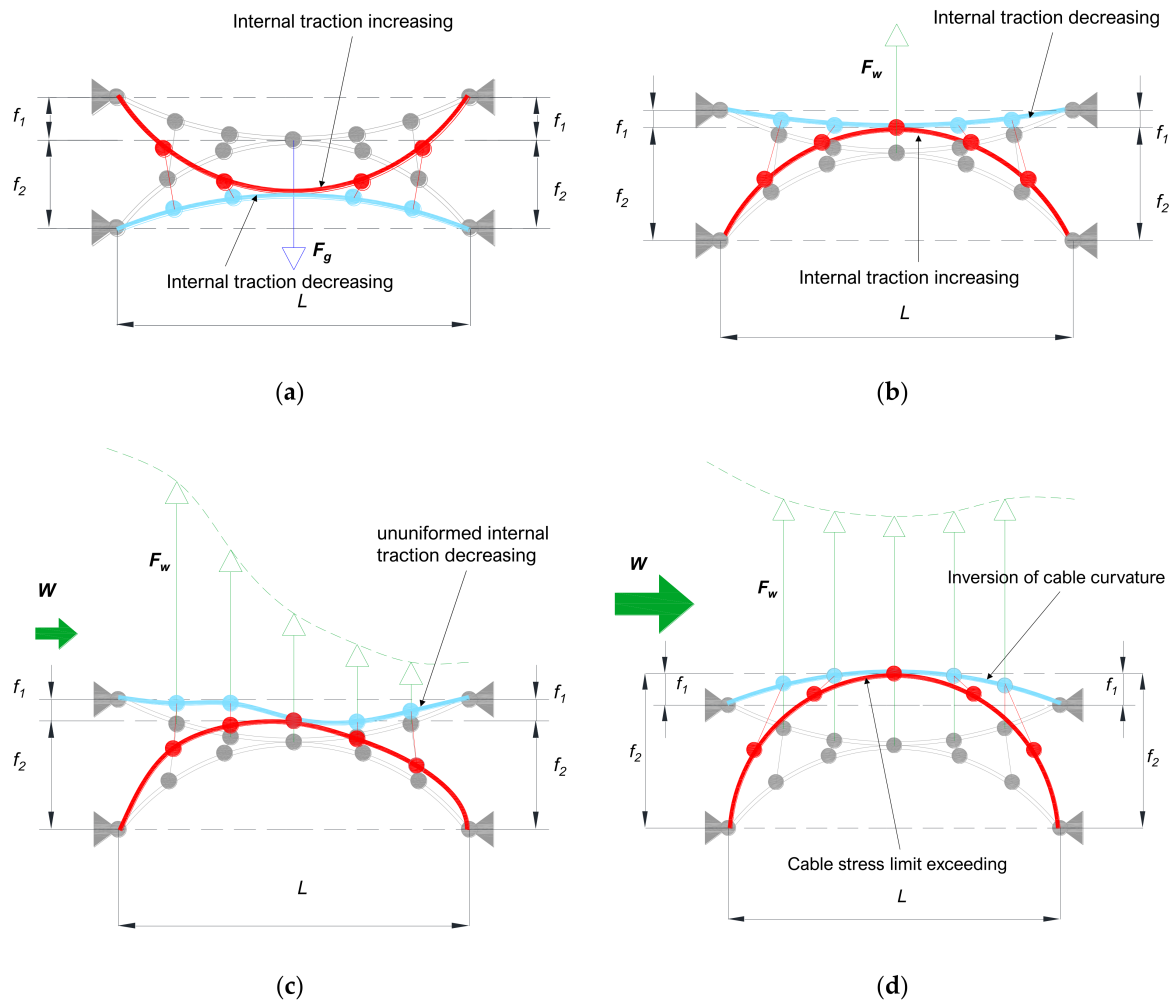


Figure 1. Structural behavior: gravitational load (a), suction (b), ununiformed suction (c), extreme suction (d).

To investigate the aeroelastic behavior of these roofs, a wind tunnel experimental campaign was conducted at the Wind Engineering Laboratory of Cracow University of Technology. A geometrical sample was selected, and six different geometries were studied. Finite Element Method geometric nonlinear analyses were performed to predict the prototype dynamics, modal frequencies and displacements under wind action [8]. Modal analyses have confirmed, as well known, that these roofs are characterized by several close natural frequencies, which makes the construction and calibration of the test model very difficult. Test models were constructed in a 1:200 geometrical scale using 39 steel ropes along L_1 and 39 steel ropes along L_2 (Figure 2a), to reproduce the prototype structural setup. In Figure 2a, f_1 and f_2 are the upward and downward cable sags, respectively, L_1 and L_2 are the upward and downward cable spans, respectively and, finally, H_1 and H_2 are the minimum and maximum roof distance from the ground.

The cable net was covered by a silk fabric to reproduce the aerodynamics. The dynamic characteristics of the model were identified by the acquisition of free (ambient) vibration at four accelerations (Figure 2b). Very small and light accelerometers were used in this research (with a weight below 1 g). In total, 49 nodes were identified for the square roof plan.

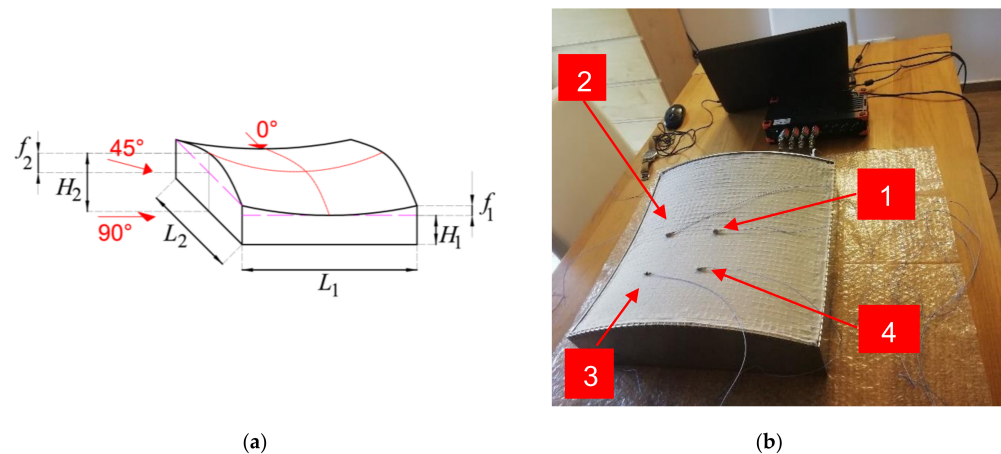


Figure 2. Geometry (a) and test model with sensor position (b) [15].

Several methods were used to identify and compare the results, such as the Welch power spectral density, the random decrement technique, empirical mode decomposition and the Frequency Domain Decomposition (FDD) [32,33]. FDD is a common output-only technique used in different structural engineering fields for dynamic identification purposes, where it can be useful for structural health monitoring due to its applicability when the input data are unknown. The FDD technique is based on approximating a complicated system response by subdividing it into independent SDOF ones that correspond to each significant mode. Further related details can be found in [15] and the next chapter. The FDD technique involves the main steps listed below:

- Spectral density matrix estimations starting from the registered raw data.
- Performing SVD of the spectral density matrices.
- If different setups of the test are available, then averages of the first singular values of all setups should be evaluated, as well as the averages of the second, etc.
- Finally, the average singular value peaks should be captured. For well-distinguished modes, the main singular value (the 1st value) should always be identified.
- Otherwise, as in the case of close or repeated modes, all singular values should be captured (the 2nd, the 3rd, etc., in addition to the 1st one).

Natural frequencies range from about 10 = to 30 Hz for each test model. The structural damping ratio was identified using both the Random Decrement Technique (RDT) and the Empirical Mode Decomposition (EMD), and it ranges from 1% to 5%. Finally, the modal deformed shapes were estimated by the Frequency Domain Decomposition (FDD). All magnitudes were scaled according to the aeroelastic scaling [34,35]. Experimental testing in the wind tunnel requires aeroelastic model scaling requirements for different geometrical aspects (i.e., dimensions, mass and inertial distribution, and stiffness and damping properties) in order to ensure consistency with the wind tunnel flow scaling. The presented criteria hereafter were adopted in this work to ensure the suitability of the models for the experiential campaign. Equation (1) defines, as a function of the geometrical scale (λ_L), the ratio of translational mass between the model and prototype (λ_m):

$$\lambda_m = \lambda_L^3 \quad (1)$$

Equation (2) instead, defines another parameter of the speed scaling as a product between the previously presented factor (λ_m) from Equation (1) and the ratio of the natural frequencies between the model and prototype (λ_η) [15]:

$$\lambda_V = \lambda_L \lambda_\eta \quad (2)$$

A geometrical scale parameter equal to 1:200 ($\lambda_m = (1/200)^3 = 1.25 \cdot 10^{-7}$) was considered for the model, taking into account the various characteristics to ensure a small value of the roof that might result in a sufficiently large fundamental frequency in addition to an effective low wind velocity at the corresponding height of the model roof (Equation (2)). The damping ratio, as a non-dimensional parameter itself, of the model should be equal to the prototype. However, the literature does not provide well-established damping values either for the cable net roof or even the membrane roof, while it gives the values only for a few specific cases [14]. Nevertheless, the membrane effect in the case of the studied roof, connecting between the cables, should increase the damping value with respect to other cases, such as suspension bridges or conventional steel structure, making it reasonable to assume a relatively higher value, which eventually has an impact on the dynamics of the tensile structure.

Various accurate considerations were taken into account for the realization of the connection between the model elements. Moreover, the choice of the material either for the representative cable net or membrane elements was made precisely in order to avoid mass distribution values that might have a strong impact on the overall dynamic behavior. Further technical details can be found in [14,15].

Free (ambient) vibration records recorded from the roof surface were used to obtain the main dynamic characteristics (frequencies + corresponding damping ratio values) of the system. In this respect, 39 monitoring points were positioned on the external surface of the roof, where four small accelerometers were alternated between the different positions following 13 distinguished patterns, as shown in Figure 3a. Each signal registration was identified by a relatively high sampling frequency (1600 Hz) and duration equal to 300 s. Figure 3b captures a 20 s window during a regular time history registration. Finally, it should be mentioned that due to the noticeably low weight of the roof structure and in order to not affect its response due to significant additional weight (e.g., accelerometer), the sensor type that was chosen and adopted in the experimental test is accelerometer model 352A24 PCB PIEZOTRONICS (extremely lightweight 0.8 g, and high sensitivity 100 mV/m/s², 1 to 8 kHz), which was attached to the roof in a careful way in order not to deform the sensitive surface of the roof (using some tiny magnets and a tape). All time histories were analyzed through a probabilistic approach to investigate the uncertainties affecting the dynamic proprieties estimation [36,37].

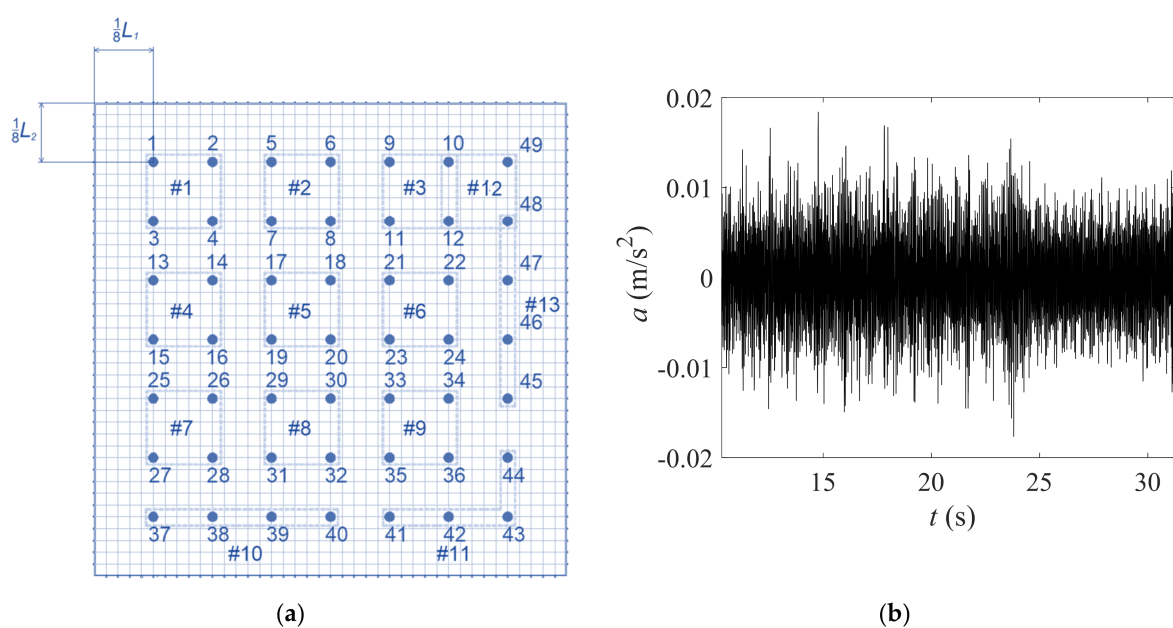


Figure 3. Test setup (a) and a typical signal (b).

3. Singular Value Decomposition Analyses

This study was focused on a square plan roof with a hyperbolic, parabolic shape roof. Referring to Figure 2a, at the model scale, f_1 was equal to 13.3 mm, f_2 was equal to 26.6 mm, L_1 and L_2 were equal to 400 mm, H_1 was equal to 66.7 mm and H_2 was equal to 106.6 mm.

In linear algebra, the Singular Value Decomposition (SVD) of a matrix is a factorization of that matrix into three matrices. This value has some interesting algebraic properties and conveys important geometrical and theoretical insights about linear transformations. It also has some important applications in data science [24–31]. Singular value decomposition takes a rectangular matrix of gene expression data (defined as A , where A is an $n \times p$ matrix) in which the n rows represent the genes, and the p columns represent the experimental conditions. The SVD theorem states:

$$A_{n \times p} = U_{n \times n} \times S_{n \times p} \times V_{p \times p}^T \tag{3}$$

where the $U_{n \times n}$ columns are the left singular vectors (gene coefficient vectors); $S_{n \times p}$ (the same dimensions as A) has singular values and is diagonal (mode amplitudes); and $V_{p \times p}^T$ has rows that are the right singular vectors (expression level vectors). The SVD represents an expansion of the original data in a coordinate system where the covariance matrix is diagonal. Calculating the SVD consists of finding the eigenvalues and eigenvectors of $A_{n \times p} \times A_{n \times p}^T$ and $A_{n \times p}^T \times A_{n \times p}$. The eigenvectors of $A_{n \times p}^T \times A_{n \times p}$ make up the columns of $V_{p \times p}$, the eigenvectors of $A_{n \times p} \times A_{n \times p}^T$ make up the columns of $U_{n \times n}$. The singular values in $S_{n \times p}$ are also square roots of eigenvalues from $A_{n \times p} \times A_{n \times p}^T$ or $A_{n \times p}^T \times A_{n \times p}$. The singular values are the diagonal entries of the $S_{n \times p}$ matrix and are arranged in descending order. The singular values are always real numbers. If matrix $A_{n \times p}$ is a real matrix, then $U_{n \times n}$ and $V_{p \times p}$ are also real.

The singular value decomposition was applied to all 49 signals acquired by ambient vibration tests, and the trend of the singular values is shown in Figure 4. Singular value matrix S was calculated, varying the number of modes, and it was observed that the trend was very similar for the first five modes. It means that the dynamics of the first five modes are robustly defined by tests using only a few sensors. On the contrary, in order to capture six or more modes, several sensors are necessary, and they should be located close to the roof borders.

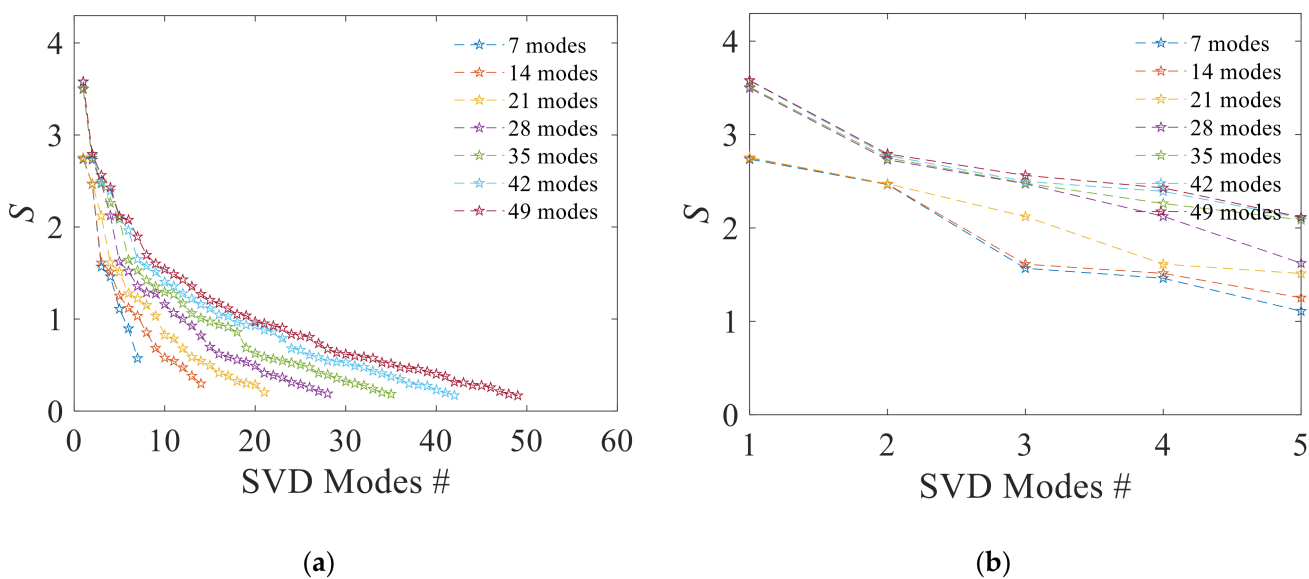


Figure 4. Singular values, S , variation depending on the number of modes: overview (a), zoom view (b).

Figures 5 and 6 show a comparison between six modes estimated by SVD (i.e., eigenvectors plot) and structural modes (i.e., test model scale) estimated by FFD.

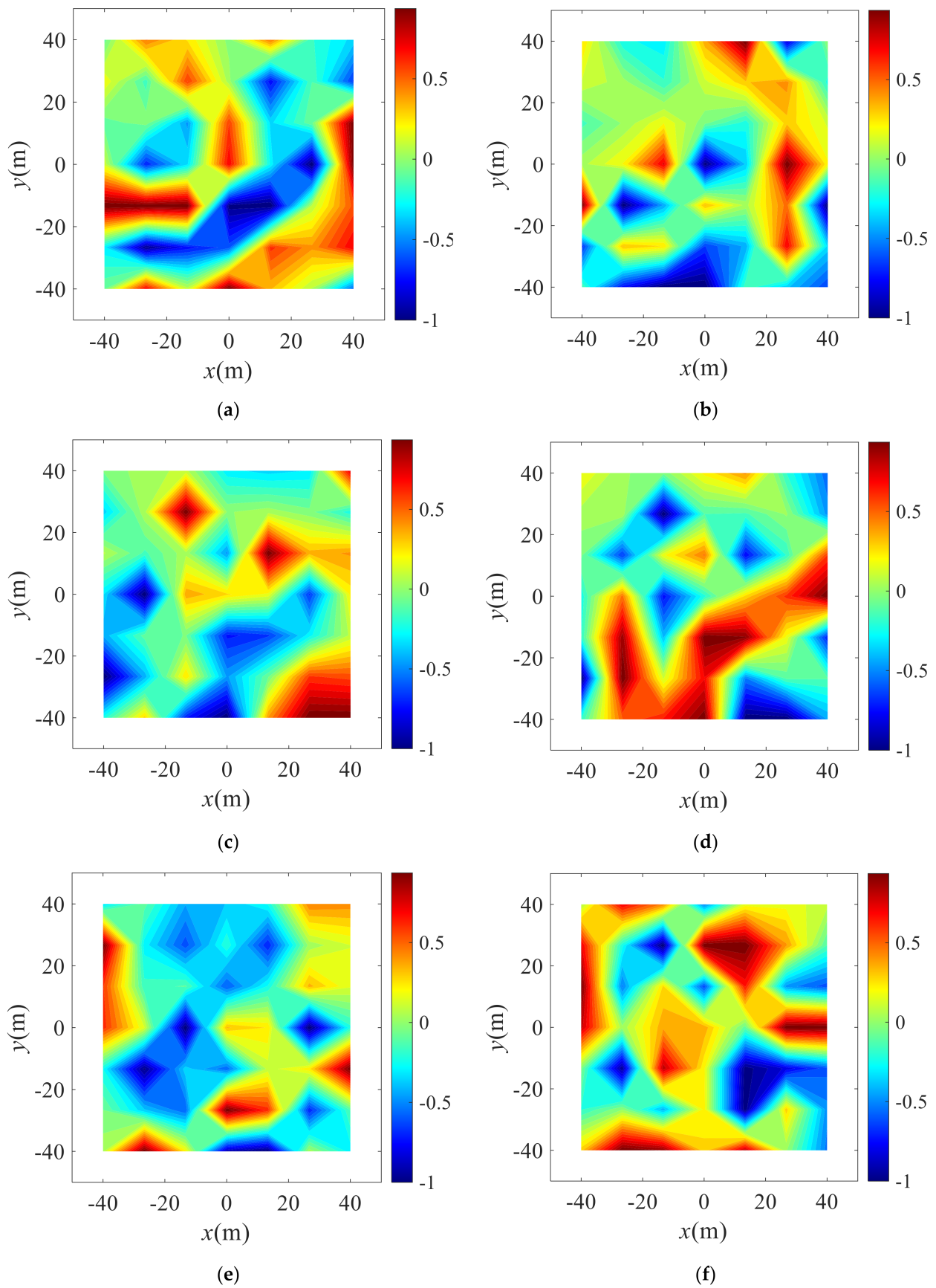


Figure 5. Eigenvectors by SVD: #1 (a), #2 (b), #3 (c), #4 (d), #5 (e) and #6 (f).

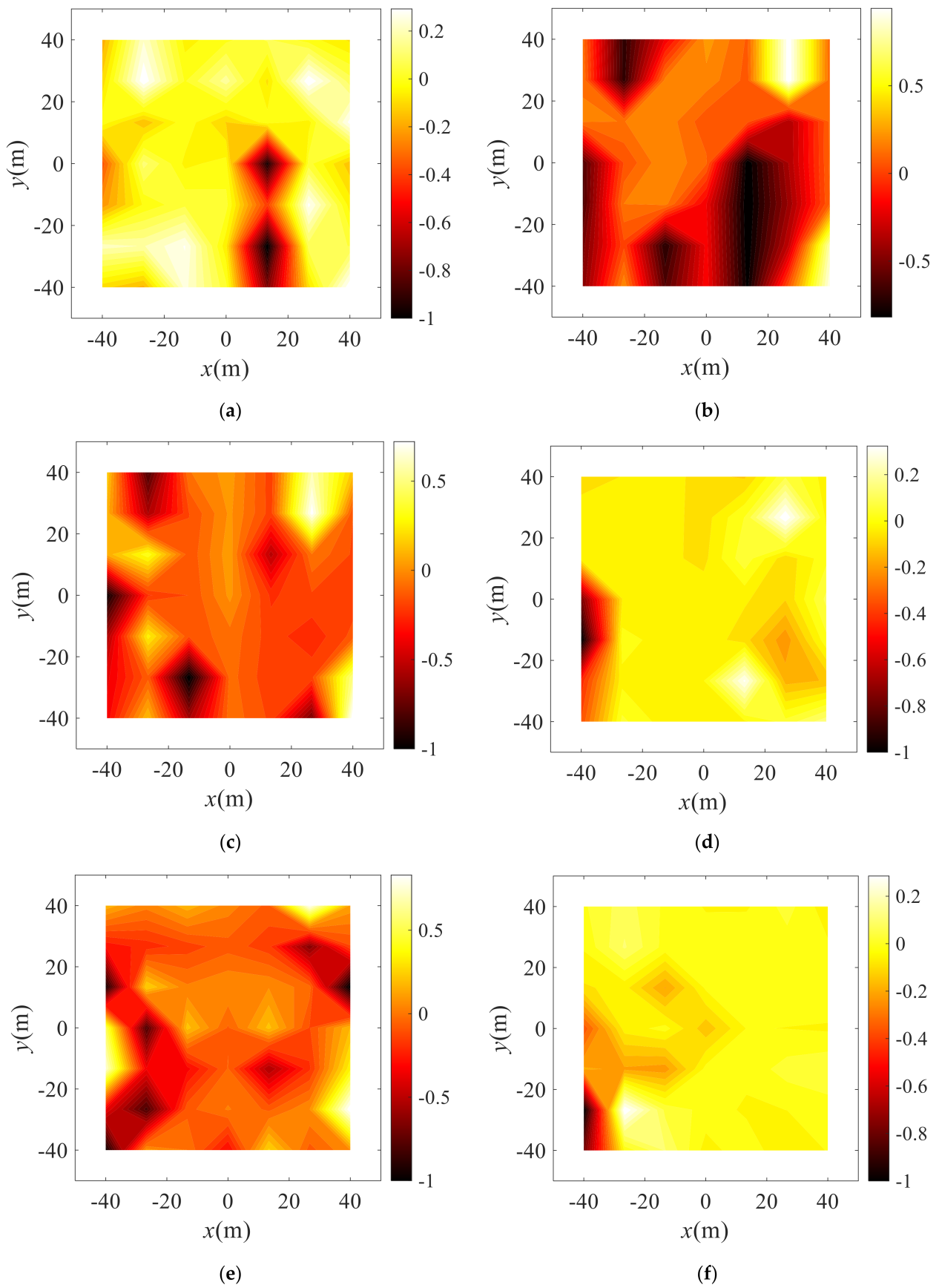


Figure 6. Structural modes by FFD: #1 (a), #2 (b), #3 (c), #4 (d), #5 (e) and #6 (f).

It was observed that, even if some peaks are similar (for example, for mode #2, Figures 5b and 6b), the global representation of modes is different. Overall, the difference between plots by FFD and SVD is significant, highlighting that the two methods should be carefully integrated. However, several considerations should be taken into account. All plots show that, in general, peaks are located around the center of the roof. Modes are mostly asymmetric, and valleys and bumps are antipolar over the roof center. This trend confirms the deformed modal shapes given by [8] and is estimated by modal analyses performed through the FEM model of cable net roofs.

4. The Spatial Correlation of Free Ambient Vibration Accelerations

Aeroelastic effects such as the large displacement field wind–structure interaction may become relevant depending on factors such as the dimensions and characteristics of the structure, as well as its flexibility. Thus, as detailed in the literature [38,39], additional nonlinear numerical analyses and ad hoc wind tunnel testing might be necessary.

In the field of dynamic identification, the correlation of the acceleration time-history records between the variant monitoring points of the roof can be a significant parameter to check the correct sensor position. Risky (i.e., unsafe) or unnecessary (i.e., redundant) design considerations of the different structural members might result from some mistakes in the evaluation process depending on their area of influence. Thus, a correlation coefficient of the ambient records time history registrations between two points (one reference point P_0 and another varying one P) on the roof can be defined according to the scientific literature as:

$$r(P, P_0) = \frac{\text{cov}(P, P_0)}{\sigma_P \sigma_{P_0}} \quad (4)$$

where σ_{P_0} and σ_P are the time-history standard deviation of the two aforementioned points P_0 and P , while $\text{cov}(P, P_0)$ is their covariance, which can be evaluated as:

$$\text{cov}(P, P_0) = E\{[c_p(P) - E(c_p(P))][c_p(P_0) - E(c_p(P_0))]\} \quad (5)$$

in which the expected value is represented by E .

Figure 7 illustrates the correlation coefficient for the same significant signals. In particular, all plots reported in Figure 7 show the correlation coefficient estimated between signal #i at position #1 and all sensors located on the roof. This plot establishes the correlation between signal #i and all acquired signals on the roof. A value equal to 1 means perfect correlation (i.e., a signal with itself), and values smaller than 0.2 mean poor correlation. Results show that each signal is minimally correlated with others. Each signal is acceptably correlated only with a signal acquired very close to it. This trend suggests an independent vibration of each sensor position and, as a consequence, an agreement with the presence of several local modes of structural vibration.

Finally, Figure 7 also shows that the best correlation between two different sensor positions occurs between positions along the y direction, which corresponds to the downward cables' alignment. This trend was observed both close to the border (Figure 7b) and in the central roof area (Figure 7c). It underlines that the structural vibration along downward cables is more correlated than along upward cables. For these reasons, a lower number of sensors along downward cables (i.e., y direction, Figure 7) as well as a relatively larger one along upward cable (i.e., x direction, Figure 7) can be used during the measurements.

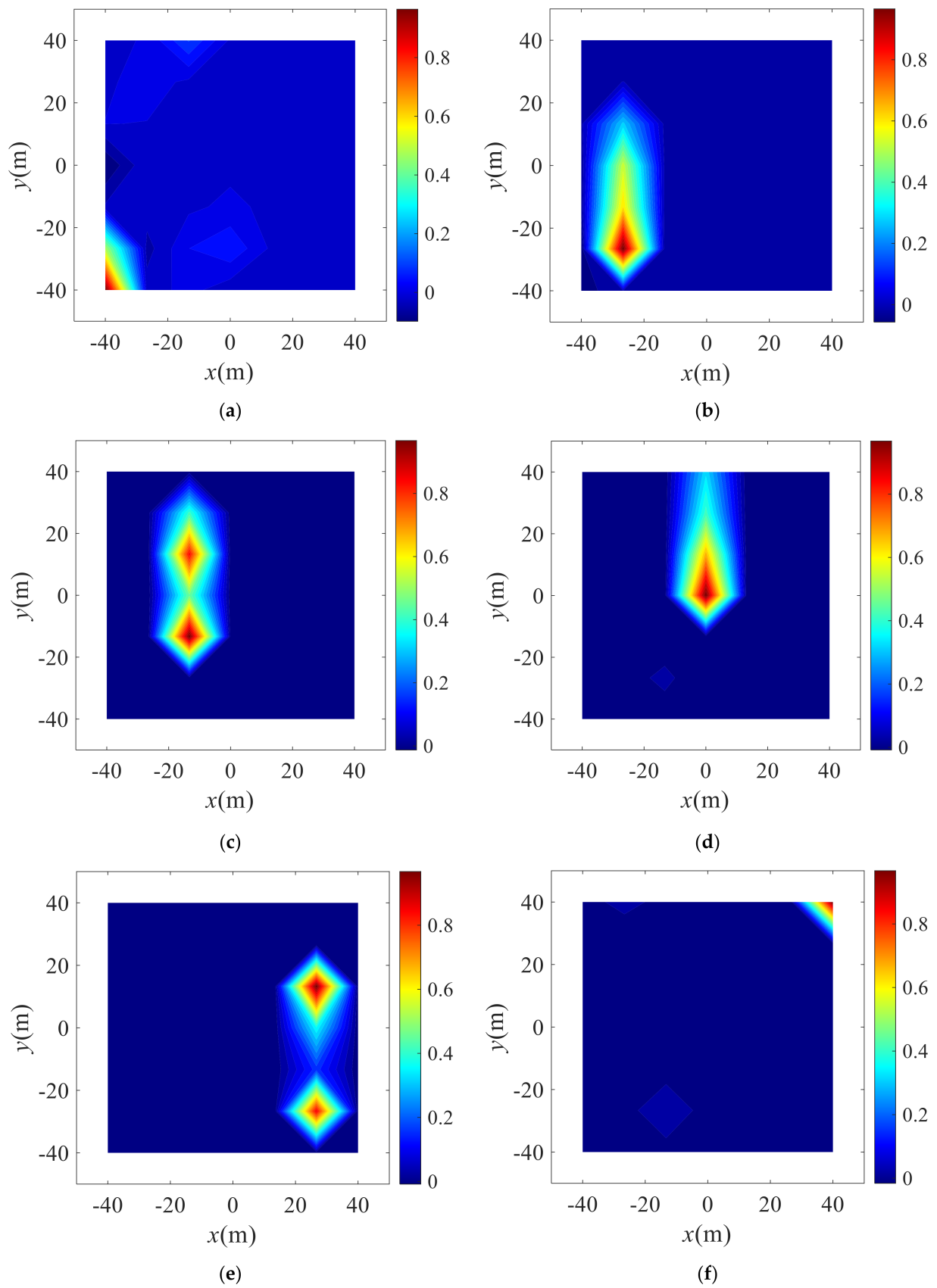


Figure 7. Correlation coefficients of the sensor #i vs. all: #37 (a), #28 (b), #29 (c), #20 (d), #22 (e) and #49 (f) (Rif. Figure 2a).

5. Conclusions

The structural modes of an aeroelastic test model of a cable net and membrane roof with a hyperbolic paraboloid shape and a square plan shape were estimated by the Singular Value Decomposition (SVD) and the Frequency Domain Decomposition (FFD). Both SVD and FFD approaches were applied to signals acquired through ambient vibration measurements. The Eigen Values trend was plotted to estimate the variability between considering only a few or several modes. It was observed that the S matrix for the first five modes is very similar, using the contribution of only seven or all signals. It means that the first five modes are robustly estimated by the test setup. The comparison between the eigenvectors plot and results given by the FFD method has shown that some peaks are similar close to the roof border, but overall, the global trend is quite different. This suggests integrating this approach to predict the test model modal deformed shapes. The double investigation through FFD and SVD gives significant knowledge of the structural dynamics: after the mode analyses by FFD, the SVD method provides the modes' significance to select them efficiently.

The correlation coefficients between signals were calculated to evaluate the suitability of the sensors' position. It was observed that signals along downward cables are more correlated than signals along upward cables; therefore, it can be recommended to use a lower number of sensors along downward cables than along upward cables in future tests.

Author Contributions: Conceptualization, F.R.; Methodology, F.R.; Formal analysis, F.R. and S.M.; Investigation, F.R., C.B., S.M., A.P., M.F.S., L.F. and R.K.; Data curation, F.R., A.P., M.F.S., L.F. and R.K.; Writing—original draft, F.R., C.B., S.M., A.P., M.F.S., L.F., R.K. and D.F.; Supervision, D.F. All authors have read and agreed to the published version of the manuscript.

Funding: This research was supported by the Italian Ministry of Education.

Institutional Review Board Statement: Not applicable.

Informed Consent Statement: Not applicable.

Data Availability Statement: The data used to support this research are available from the corresponding author upon request.

Acknowledgments: This research was supported by the Polish government through the Scholarship of the Polish National Agency for Academic Exchange (NAWA project, PPN/ULM/2020/1/00085). Model construction: Maria Rita Guerrieri deserves to be thanked for her collaboration during experiments. The authors would like to thank the Multiassetlab.srl staff and Davide Perazzetti for their support during the model construction.

Conflicts of Interest: The authors declare no conflict of interest.

References

1. Rizzo, F.; Barbato, M.; Sepe, V. Shape dependence of wind pressure peak factor statistics in hyperbolic paraboloid roofs. *J. Build. Eng.* **2021**, *44*, 103203. [[CrossRef](#)]
2. Rizzo, F.; Barbato, M.; Sepe, V. Peak factor statistics of wind effects for hyperbolic paraboloid roofs. *Eng. Struct.* **2018**, *173*, 313–330. [[CrossRef](#)]
3. Rizzo, F.; Zazzini, P. Shape dependence of acoustic performances of buildings with a hyperbolic paraboloid cable net membrane roof. *J. Acoust. Aust.* **2017**, *45*, 421–443. [[CrossRef](#)]
4. Rizzo, F.; Zazzini, P. Improving the acoustical properties of an elliptical plan space with a cable net membrane roof. *J. Acoust. Aust.* **2016**, *44*, 449–456. [[CrossRef](#)]
5. Rizzo, F.; Sepe, V. Static loads to simulate dynamic effects of wind on hyperbolic paraboloid roofs with square plan. *J. Wind Eng. Ind. Aerodyn.* **2015**, *137*, 46–57. [[CrossRef](#)]
6. Rizzo, F.; Sepe, V.; Ricciardelli, F.; Avossa, A.M. Wind pressures on a large span canopy roof. *Wind. Struct.* **2020**, *30*, 299–316. [[CrossRef](#)]
7. Colliers, J.; Degroote, J.; Mollaert, M.; De Laet, L. Mean pressure coefficient distributions over hyperbolic paraboloid roof and canopy structures with different shape parameters in a uniform flow with very small turbulence. *Eng. Struct.* **2020**, *205*, 110043. [[CrossRef](#)]
8. Vassilopoulou, I.; Gantes, C.J. Influence of a Deformable Contour Ring on the Nonlinear Dynamic Response of Cable Nets. *Structures* **2016**, *6*, 146–158. [[CrossRef](#)]

9. Vassilopoulou, I.; Petrini, F.; Gantes, C.J. Nonlinear Dynamic Behavior of Cable Nets Subjected to Wind Loading. *Structures* **2017**, *10*, 170–183. [CrossRef]
10. Colliers, J.; Mollaert, M.; Vierendeels, J.; De Laet, L. Collating Wind Data for Doubly-curved Shapes of Tensioned Surface Structures (Round Robin Exercise 3). *Procedia. Eng.* **2016**, *155*, 152–162. [CrossRef]
11. Rizzo, F.; Ricciardelli, F. Design pressure coefficients for circular and elliptical plan structures with hyperbolic paraboloid roof. *Eng. Struct.* **2017**, *139*, 153–169. [CrossRef]
12. Rizzo, F.; Caracoglia, L. Examination of Artificial Neural Networks to predict wind-induced displacements of cable net roofs. *Eng. Struct.* **2021**, *245*, 112956. [CrossRef]
13. Liu, M.; Chen, X.; Yang, Q. Characteristics of dynamic pressures on a saddle type roof in various boundary layer flows. *J. Wind Eng. Ind. Aerodyn* **2016**, *150*, 1–14. [CrossRef]
14. Rizzo, F.; Kopp, A.G.; Giaccu, G. Investigation of wind-induced dynamics of a cable net roof with aeroelastic wind tunnel tests. *Eng. Struct.* **2021**, *229*, 111569. [CrossRef]
15. Rizzo, F.; Sadhu, A.; Abasi APistol, A.; Flaga, L.; Venanzi, I.; Ubertini, F. Construction and dynamic identification of aeroelastic test models for flexible roofs. *Archiv. Civ. Mech. Eng.* **2023**, *23*, 16. [CrossRef]
16. CEN—EN1991-1-4; Eurocode1: Actions on Structures Part 1–4: General Actions—Wind Actions. CEN: Bruxelles, Belgium, 2005.
17. AIJ (Architectural Institute of Japan). Chapter 6: Wind Loads. In *Recommendations for Loads on Buildings*; AIJ: Tokyo, Japan, 2004.
18. SIA (Swiss Society of Engineers and Architects). *Action on Structures—Appendix C: Force and Pressure Factors for Wind.*; SIA: Baukultur, Switzerland, 2003; Volume 261.
19. Krishna, P.; Kumar, K.; Bhandari, N.M. *Wind Loads on Buildings and Structures. Indian Standard IS:875, Part 3, Proposed Draft & Commentary. Random data Analysis and Measurement Procedures*, 3rd ed.; Bendat, J.S., Piersol, A.G., Eds.; John Wiley and Sons: New York, NY, USA, 2000.
20. ISO 4354:2009; Wind Action on Structures—D.3 Wind Tunnel Testing Procedures. ISO (International Standards Organization): London, UK, 2012.
21. NRC/CNRC (National Research Council/Conseil National de Recherches Canada). *Commentary to the National Building Code of Canada, Commentary I: Wind Load and Effects*; NRC/CNRC: Ottawa, ON, Canada, 2010.
22. Brincker, R.; Zhang, L.; Andersen, P. Modal identification of output-only systems using frequency domain. *Smart Mater. Struct.* **2001**, *10*, 441–445. [CrossRef]
23. Brincker, R.; Zhang, L.; Andersen, P. Modal Identification from Ambient Response Using Frequency Domain Decomposition. In Proceedings of the 18th International Modal Analysis Conference, San Antonio, TX, USA, 7–10 February 2000.
24. Biglieri, E.; Yao, K.; Angeles, L. Some properties of SVD and their application to digital signal processing. *Signal Process.* **1989**, *19*, 277–289. [CrossRef]
25. Teukolsky, S.A.; Vetterling, W.T.; Flannery, B.P. *Numerical Recipes in C: The Art of Scientific Computing*; Cambridge University Press: Cambridge, UK, 1997.
26. Ciarlet, P.G. *Introduction to Numerical Linear Algebra and Optimization*; Cambridge University Press: Cambridge, UK, 1989.
27. Li, Y.; Huang, H.; Zhang, W.; Sun, L. Structural full-field responses reconstruction by the SVD and pseudo-inverse operator-estimated force with two-degree multi-scale models. *Eng. Struct.* **2021**, *249*, 112986. [CrossRef]
28. Wang, P.; Zhou, W.; Li, H. A singular value decomposition-based guided wave array signal processing approach for weak signals with low signal-to-noise ratios. *Mech. Syst. Signal Process.* **2020**, *141*, 106450. [CrossRef]
29. Sun, G.; Li, W.; Luo, Q.; Li, Q. Thin-Walled Structures Modal identification of vibrating structures using singular value decomposition and nonlinear iteration based on high-speed digital image correlation. *Thin-Walled Struct.* **2021**, *163*, 107377. [CrossRef]
30. Luo, J.; Liu, G.; Huang, Z.; Law, S.S. Mode shape identification based on Gabor transform and singular value decomposition under uncorrelated colored noise excitation. *Mech. Syst. Signal Process.* **2019**, *128*, 446–462. [CrossRef]
31. Sadeqi, A.; Moradi, S. A new SVD-based filtering technique for operational modal analysis in the presence of harmonic excitation and noise. *J. Sound Vib.* **2021**, *510*, 116252. [CrossRef]
32. Farshchin, M. Frequency Domain Decomposition (FDD). 2022. Available online: <https://www.mathworks.com/matlabcentral/fileexchange/50988-frequency-domain-decomposition-fdd> (accessed on 11 October 2022).
33. Tamura, Y.; Yoshida, A.; Zhang, L.; Ito, T.; Nakata, S. Examples of modal identification of structures in Japan by FDD and MRD techniques. In Proceedings of the EACWE4—The Fourth European & African Conference on Wind Engineering, Prague, Czech Republic, 11–15 July 2005.
34. Isyumov, N. The Aeroelastic Modelling of Tall Buildings. In Proceedings of the International Workshop on Wind Tunnel Modelling Criteria and Technique in Civil Engineering Applications, Gaithersburg, MD, USA, 14–16 April 1982.
35. Rizzo, F.; Caracoglia, L.; Piccardo, G. Examining wind-induced floor accelerations in an unconventionally shaped, high-rise building for the design of smart screen walls. *J. Build. Eng.* **2021**, *43*, 103115. [CrossRef]
36. Rizzo, F.; Ricciardelli, F.; Maddaloni, G.; Bonati, A.; Occhiuzzi, A. Experimental error analysis of dynamic properties for a reduced-scale high-rise building model and implications on full-scale behaviour. *J. Build. Eng.* **2020**, *28*, 101067. [CrossRef]
37. Rizzo, F.; Huang, M. Peak value estimation for wind-induced lateral accelerations in a high-rise building. *Struct. Infrastruct. Eng.* **2021**, *9*, 1317–1333. [CrossRef]

38. Rizzo, F.; Sepe, V.; Vasta, M. Correlation structure of wind-tunnel pressure fields for a hyperbolic paraboloid roof. In Proceedings of the AIMETA 2017—XXIII Conference of the Italian Association of Theoretical and Applied Mechanics, Salerno, Italy, 4–7 September 2017; pp. 462–471.
39. Rizzo, F.; Sepe, V.; Sabbà, M.F. Investigation of the Pressure Coefficients Correlation Field for Low-Rise Building Roofs. *Appl. Sci.* **2022**, *12*, 10790. [[CrossRef](#)]

Disclaimer/Publisher’s Note: The statements, opinions and data contained in all publications are solely those of the individual author(s) and contributor(s) and not of MDPI and/or the editor(s). MDPI and/or the editor(s) disclaim responsibility for any injury to people or property resulting from any ideas, methods, instructions or products referred to in the content.